

# Experimental Study of the Pressure Generated by a Linear Heat Source in a Semi-ventilated Enclosure

Kouéni-Toko Christian Anicet<sup>1,\*</sup>, Patte-Rouland Béatrice<sup>2</sup>, Paranthoën Pierre<sup>2</sup>

<sup>1</sup>Department of Renewable Energy, National Advanced School of Engineering of Maroua, University of Maroua, Maroua, Cameroon

<sup>2</sup>CNRS UMR 6614 CORIA, University Boulevard, Saint-Etienne du Rouvray, France

## Email address:

christiandrakoueni@gmail.com (Kouéni-Toko C. A.)

\*Corresponding author

## To cite this article:

Kouéni-Toko Christian Anicet, Patte-Rouland Béatrice, Paranthoën Pierre. Experimental Study of the Pressure Generated by a Linear Heat Source in a Semi-ventilated Enclosure. *Engineering and Applied Sciences*. Vol. 7, No. 1, 2022, pp. 8-15. doi: 10.11648/j.eas.20220701.12

**Received:** February 12, 2022; **Accepted:** March 2, 2022; **Published:** March 9, 2022

---

**Abstract:** The objective of this work is to understand and successfully control the phenomena found at the openings when the enclosure is subjected to a linear heat source. The enclosure is not adiabatic. The control and understanding of its phenomena will be carried out by differential static pressure measurements. These measurements were carried out in calm weather using a Furness control micro-manometer in 20 points at positions  $x^+ = 0$ ,  $y^+ = -0.5$  and along the vertical  $z^+$ . We have studied four enclosure configurations. Each configuration has two or four or six openings. The openings have identical characteristics, height  $h = 34$  mm and width  $l = 210$  mm. The height of the enclosure is  $H = 520$  mm and the length is equal to the width  $L = l = 210$  mm. We have shown the influences of the reduced Grashof number ( $Gr^*$ ), the number and the position of the openings on the differential static pressure with and without dimension and compared the experimental results obtained with those of cases 11 and 12 of Kouéni Toko (2019). It appears that the values and forms of the static pressure and the values of the neutral height can vary according to  $Gr^*$  and number and the position of the openings.

**Keywords:** Enclosure, Semi-ventilated, Linear Heat Source, Pressure Profile

---

## 1. Introduction

Natural convection is the set of movements caused by internal forces in fluids. In this convection, the difference in density which is most of the time caused by the temperature difference with the force of gravity creates a buoyancy force which therefore creates a difference in momentum. The study of natural convection in enclosures with at least one opening can generate the movements of fluid at the level of the opening (s) [1–5]. In this situation we can speak of natural ventilation [6–14]. José Luis Fernández-Zayas *et al.* [15] have performed an experimental analysis of natural ventilation of an office building in Mexico city.

The study of natural ventilation in semi-confined enclosures has been the subject of a large number of theoretical, experimental and numerical works. In particular that of Linden, Lane-Serff and Smeed [1], who studied the case of a point source of buoyancy placed in an enclosure having two openings, height  $H$  and radius  $R$ , with an aspect

ratio  $H/R < 1$ . They showed that there is a displacement regime and that stratification develops characterized by two layers separated by an interface. Kaye and Hunt [2], studied the same type of situation in the case of a rectangular enclosure presenting a heat source located at the bottom of the enclosure and two openings located at the base and at the top. They have shown that the steady state depends on two times: the filling time and the emptying time. For aspect ratios of  $1 < H/R < 5.8$ , Kaye and Hunt [7], have shown that the windings appear near the walls and induce an additional entrainment of air which has the effect of thickening the top layer (uniform temperature layer). Jeremy and Woods [10] investigated in laboratory experiments the transient filling of a room with buoyant fluid when a doorway connects the room to a large reservoir of dense fluid. And shown that the filling time has the expression  $(A/wH) \times (H/g')^{1/2}$ . Fitzgerald and Woods [16] studied theoretically and experimentally the natural ventilation of a room with a heat source at the base and with vents at multiple heights. They showed through the determination of neutral buoyancy that air enters through the

vents below the neutral buoyancy position and exits through the vents above. When a room is heated by a point source, a vertically stratified environment develops and the neutral buoyancy surface is higher than for a distributed source. To create the buoyancy force in semi-confined enclosures, previous authors who worked on natural ventilation used a fluid source in water or air. The following authors have used a solid hot source in air.

Koueni Toko [3] studied experimentally, analytically and numerically, the temperature fields in an enclosure with two low openings, heated by a linear heat source (case 11). He showed that, when a constant temperature  $\Delta T_0$  is imposed at the level of the heat source and in a steady state, the thermal plume in the enclosure was symmetrical and that at each opening, an entry of fresh air is observed at the bottom and a hot gas out let at the top.

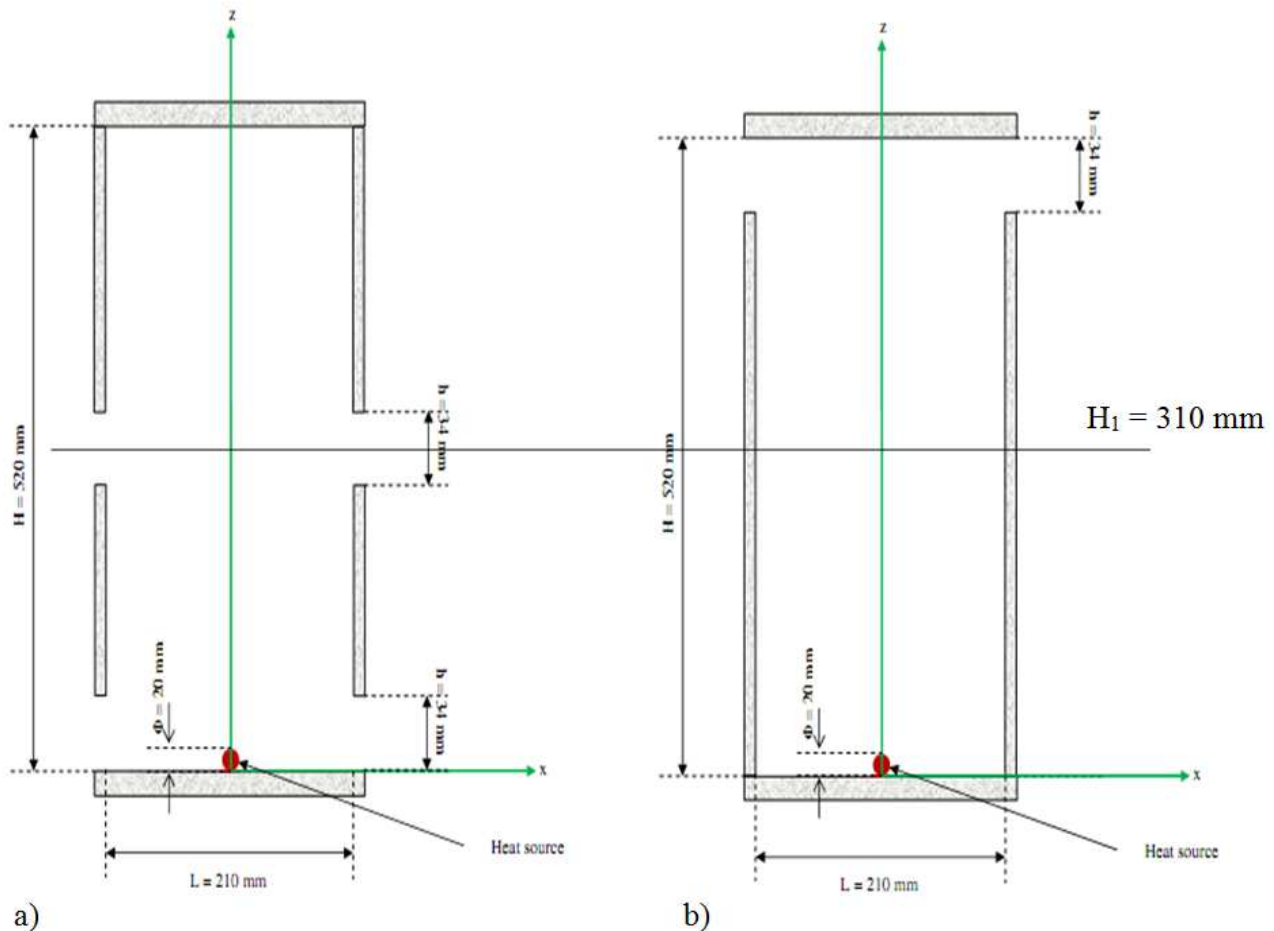
The interest of such studies lies in their involvement in many industrial applications such as cooling of electronic components, building heaters, compartment fires, etc. We will experimentally study the pressure profiles generated in a rectangular chamber with aspect ratio  $H/L = 2.476$ , heated by a linear heat source and having at least two openings. Regarding this work, Koueni Toko [3] showed in two configurations: when the enclosure has two low openings symmetrical with respect to the axis (0z) (case 11) and four openings including two located on the floor and two on the

ceiling symmetrical with respect to the axis (0z) (case 12). In these two configurations, the enclosures are heated by a linear heat source with a diameter of 20 mm. That when a constant temperature  $\Delta T_0$  is imposed at the level of the heat source and in a steady state, the differential static pressure profiles do not look the same in the two configurations.

The objective of this work is to understand and successfully control the phenomena found at the openings when the enclosure is subjected to a linear heat source. We will show the influence of the reduced Grashof number ( $Gr^*$ ), the number and the position of the openings on the differential static pressure. And compare its experimental results with the experimental and numerical results of cases 11 and 12 [3]. This study will be carried out in steady state.

## 2. Experimental Device

The experimental model (Figure 1) is of parallelepiped shape with several openings, the number of which on each side wall parallel to the heat source is 01 (cases 2, 3), 02 (case 1) and 03 (case 4). These openings have a width  $l = 210$  mm and a height of 34 mm. The model has a length equal to the width ( $l = W = 210$  mm), a height  $H = 520$  mm and is made of Plexiglas material. The model's floor and ceiling are 14 mm thick and the side walls are 8 mm. The model panels are assembled with glue.



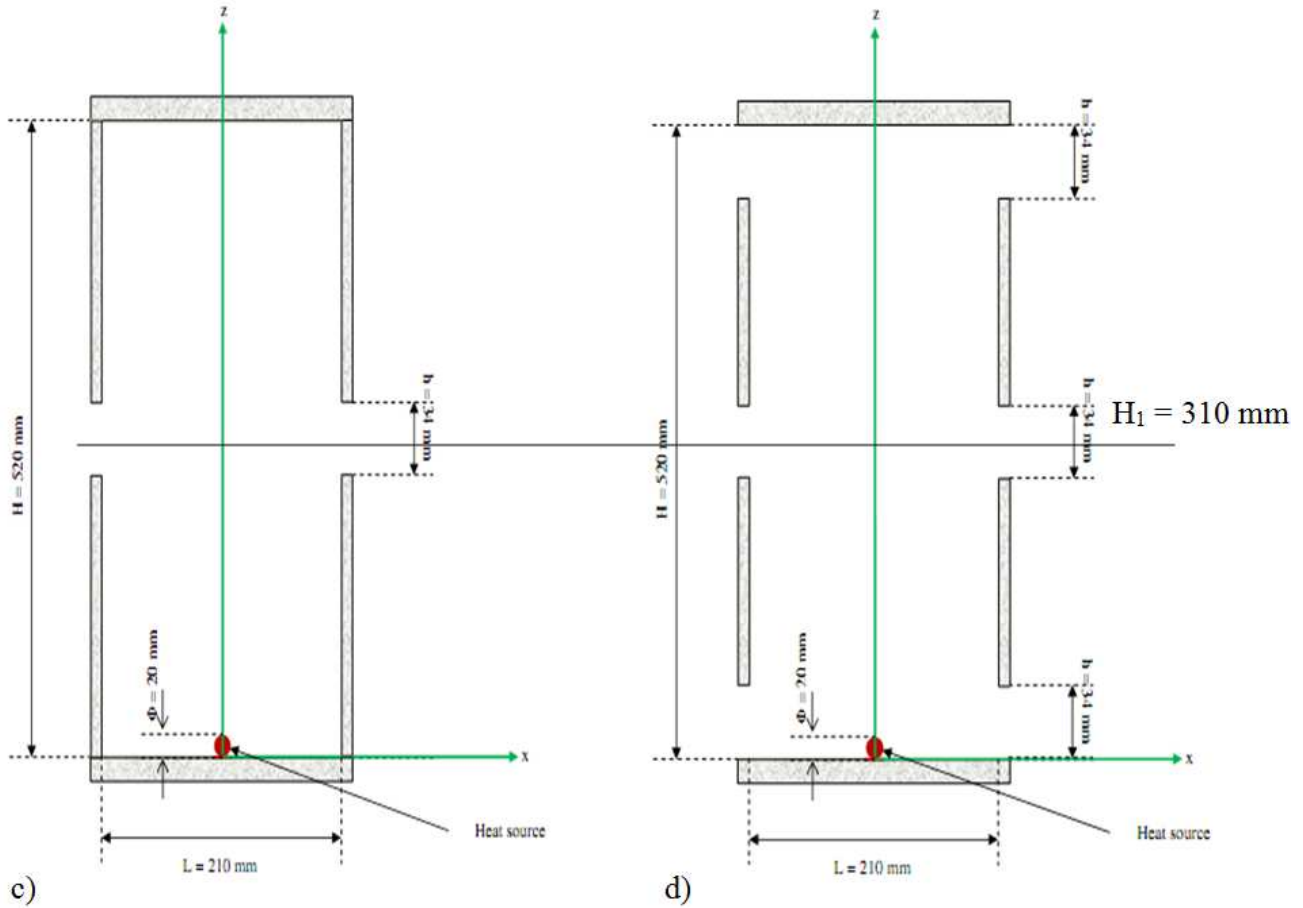


Figure 1. Experimental device a) case 1, b) case 2, c) case 3, d) case 4.

The model is three-dimensional and at an orthonormal frame of reference with axes  $Ox$ ,  $Oy$  and  $Oz$ , the origin of the frame is  $O$ .

The model is heated by a heat source of cylindrical shape with a circular base section with a diameter  $D_0 = 20 \text{ mm}$  and a length  $l_0 = 200 \text{ mm}$ . This heat source is oriented parallel to the  $Oy$  axis, at  $x = 0$  and is fixed by two stainless ropes 2 mm above the floor.

The temperature in the enclosure is almost homogeneous and equal to the outside temperature. The model is placed on a metal table. The temperature of its floor is therefore equal to the temperature of the table, on this wall, we have a Dirichlet temperature. The walls other than the floor are in contact with the air outside the enclosure. On these walls we have the Neumann condition.

The semi-confined enclosures are housed in a large, almost closed room measuring  $4\text{m} \times 4\text{m} \times 3\text{m}$  comprising two doors measuring  $0.9\text{m} \times 2\text{m}$  and  $1.6\text{m} \times 2\text{m}$  and a window measuring  $3\text{m} \times 1\text{m}$ . During the realization of the pressure and temperature measurements, we had constraints with regard to the variability of the external climatic conditions which could influence the temperature of the room. Since the measurements are carried out in natural convection and the exciter parameter of the natural convection movements in the enclosures being the temperature variation, we chose to perform the experiments in calm weather. The outside pressure was controlled by a manometer and the outside

temperature by a thermocouple placed near the enclosure.

To neglect the influence of possible variation in the outside temperature, we measured temperature differences (difference between the temperature of the enclosure and that of the external environment) and pressure differences (difference between the pressure in the enclosure at a given height and that of the external environment at the same height).

Before switching on the heating, the enclosure is in equilibrium with the external environment. Therefore, the difference between the pressure inside and outside of the enclosure at the apertures is equal to 0.

The thermocouple placed 2 mm above the heat source indicates its temperature noted  $T_0$ .  $\Delta T_0 = T_0 - T_{\text{ext}}$  is the temperature difference between the heat source and the environment outside the enclosure. The values of this temperature difference chosen for this work are 25, 40, 60 K.

The temperature  $\Delta T_0$  is kept constant by means of a self-adjusting thermal regulator by step response. The Gammadue series universal regulator used is a PID-ADVANCE regulator with two degrees of freedom, without put limitation (P: Proportional, I: Integral and D: Derivated). It has three outputs: a relay or triac output, a logic output and an analog output. The auto-tuning of this regulator is carried out by fuzzy logic with automatic selection of the calculation mode. This regulator is self-regulating or self-adapting for a permanent optimization of the regulation.

### 3. Differential Pressure Measurement and Mathematical Formulation Procedure

#### 3.1. Differential Pressure Measurement

The differential pressure measurements  $\Delta P_i(z)$  were made in the enclosure using a micro-manometer FCO14 of English Furness Control's society. This device can measure very small pressure differences in the range 0.01–10 Pa.

$$\Delta P_i(z) = P_{int}(z) - P_{ext}(z) \quad (1)$$

In order to be able to successively measure the differential pressure at different heights with a single micro-manometer, we used a Furness Control type FCS421 scanner. This selection box allow sup to twenty different wall pressure taps to be connected to the same micro-manometer. However, having only one micro-manometer, this procedure requires about fifteen minutes to carry out ten measurement points. The differential pressure measurement was performed at position  $x+ = 0$  (Figure 2).

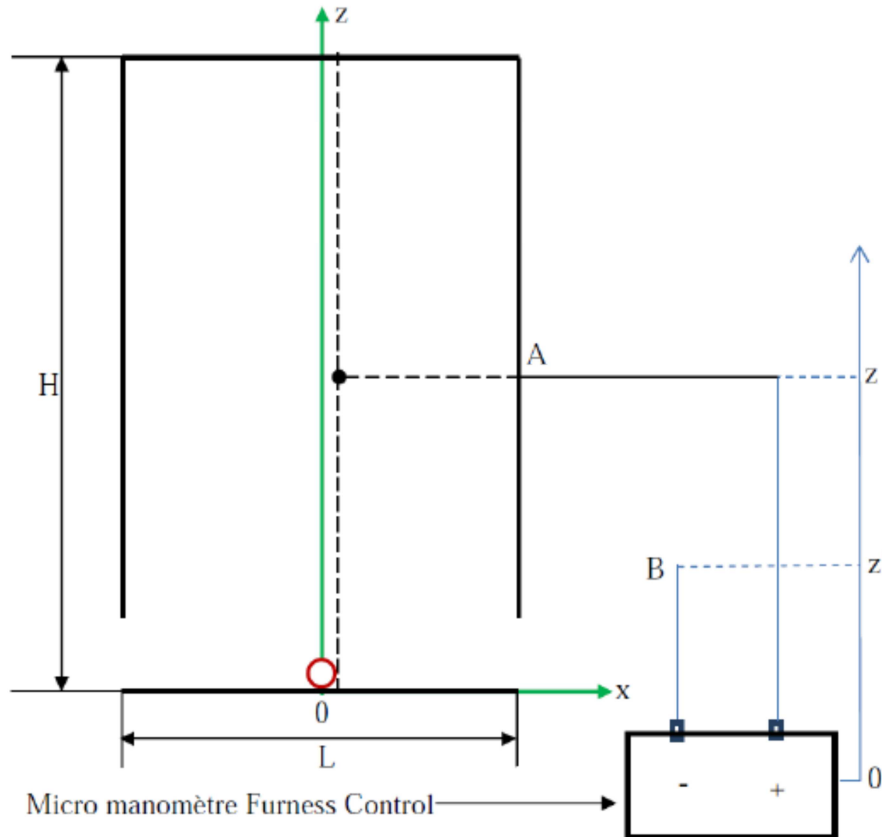


Figure 2. Differential pressure measurement.

#### 3.2. Mathematical Formulation

The simplifying assumptions used in this mathematical formulation make it possible to obtain a simplified and representative mathematical model of the physical phenomenon studied. It was assumed that the mass flow entering the enclosure is equal to that leaving, the fluid is Newtonian and compressible. The heat source has a time constant. For it to reach its set temperature, it takes some time. Measurements of differential static pressures are made when the temperature of the heat source is substantially constant. It was also assumed that the heat transfer by radiation is negligible and that the air density obeys the Boussinesq approximation in the buoyancy term as well as the dissipated power density is very low.

Equation 2 represents the steady-state mass conservation

equation [3]:

$$\rho \left( \frac{\partial u}{\partial x} + \frac{\partial v}{\partial y} + \frac{\partial w}{\partial z} \right) = 0 \quad (2)$$

The components of the velocity field are  $u$ ,  $v$ ,  $w$ .

The momentum conservation equations along the axes  $x$ ,  $y$ ,  $z$ , take into consideration the Boussinesq's approximation. These equations are established by considering that  $\frac{\rho_\infty}{\rho} \approx 1$  and that the density variations overtime and space are negligible [3]. Therefore, the momentum conservation equations established for a stationary Newtonian compressible fluid is similar to the momentum conservation equations for a stationary Newtonian incompressible fluid. These momentum conservation equations are represented by Equation 3.

$$\begin{cases} u \frac{\partial u}{\partial x} + v \frac{\partial u}{\partial y} + w \frac{\partial u}{\partial z} = -\frac{1}{\rho} \frac{\partial P}{\partial x} + \nu \left( \frac{\partial^2 u}{\partial x^2} + \frac{\partial^2 u}{\partial y^2} + \frac{\partial^2 u}{\partial z^2} \right) \\ u \frac{\partial v}{\partial x} + v \frac{\partial v}{\partial y} + w \frac{\partial v}{\partial z} = -\frac{1}{\rho} \frac{\partial P}{\partial y} + \nu \left( \frac{\partial^2 v}{\partial x^2} + \frac{\partial^2 v}{\partial y^2} + \frac{\partial^2 v}{\partial z^2} \right) \\ u \frac{\partial w}{\partial x} + v \frac{\partial w}{\partial y} + w \frac{\partial w}{\partial z} = -\frac{1}{\rho} \frac{\partial P}{\partial z} + \nu \left( \frac{\partial^2 w}{\partial x^2} + \frac{\partial^2 w}{\partial y^2} + \frac{\partial^2 w}{\partial z^2} \right) - g\beta(T - T_{ext}) \end{cases} \quad (3)$$

With

$$\frac{\partial P}{\partial z} = \frac{\partial(P' - P_0)}{\partial z} \quad (4)$$

$$P_0 = P_{0i} - \rho_0 g z \quad (5)$$

$$P' = P'_i - \rho g z \quad (6)$$

$$\frac{\partial P_0}{\partial z} = -\rho_0 g z \quad (7)$$

$$\frac{\partial P'}{\partial z} = -\rho g z, \frac{\partial(P' - P_0)}{\partial z} = (\rho_0 - \rho) \quad (8)$$

Where

$P_0$ : Pressure outside of the enclosure;

$\rho_0 = 1,2 \text{ kg.m}^{-3}$ : Density of air outside the enclosure, It has been determined for a reference temperature of 300K;

$P'$ : Pressure at the interior in the enclosure;

$\rho$ : Density of the air inside the enclosure;

$g\beta(T - T_{ext})$ : Buoyancy force generated by the heat source. This force varies because the local temperature varies.

The dimensionless conservation equations 10 and 11 are those of mass and momentum [3].

$$x^+ = \frac{x}{L}, y^+ = \frac{y}{L}, z^+ = \frac{z}{H}, u^+ = \frac{u}{U_0}, v^+ = \frac{v}{U_0},$$

$$w^+ = \frac{w}{U_0}, T^+ = \frac{T - T_{ext}}{T_0 - T_{ext}}, \text{ et } P^+ = \frac{P}{|P_{max}|}$$

With

$$U_0 = \sqrt{\frac{P_{max}}{\rho_\infty}} \quad (9)$$

The maximum velocity air inlet cool into the enclosure when the heat source is at a temperature  $\Delta T_0$ .

$$\delta = \frac{L}{H} = \frac{1}{2,476}: \text{ The inverse of aspect ratio;}$$

$$Gr = \frac{g\beta H^3 (T_0 - T_{ext})}{\nu^2}: \text{ The Grashof number;}$$

$$Gr^* = \delta^2 Gr: \text{ The Grashof number reduced.}$$

The equations 10 and 11 are respectively conservation equations of momentum and mass dimensionless [3].

$$\rho \left( \frac{1}{\delta} \frac{\partial u^+}{\partial x^+} + \frac{1}{\delta} \frac{\partial v^+}{\partial y^+} + \frac{\partial w^+}{\partial z^+} \right) = 0 \quad (10)$$

$$\begin{cases} \frac{u^+}{\delta} \frac{\partial u^+}{\partial x^+} + \frac{v^+}{\delta} \frac{\partial u^+}{\partial y^+} + w^+ \frac{\partial u^+}{\partial z^+} = -\frac{1}{\delta} \frac{\partial P^+}{\partial x^+} + \frac{1}{Gr^{*1/2}} \left( \frac{\partial^2 u^+}{\partial x^{+2}} + \frac{\partial^2 u^+}{\partial y^{+2}} + \delta \frac{\partial^2 u^+}{\partial z^{+2}} \right) \\ \frac{u^+}{\delta} \frac{\partial v^+}{\partial x^+} + \frac{v^+}{\delta} \frac{\partial v^+}{\partial y^+} + w^+ \frac{\partial v^+}{\partial z^+} = -\frac{1}{\delta} \frac{\partial P^+}{\partial y^+} + \frac{1}{Gr^{*1/2}} \left( \frac{\partial^2 v^+}{\partial x^{+2}} + \frac{\partial^2 v^+}{\partial y^{+2}} + \delta \frac{\partial^2 v^+}{\partial z^{+2}} \right) \\ \frac{u^+}{\delta} \frac{\partial w^+}{\partial x^+} + \frac{v^+}{\delta} \frac{\partial w^+}{\partial y^+} + w^+ \frac{\partial w^+}{\partial z^+} = -\frac{1}{\delta} \frac{\partial P^+}{\partial z^+} + \frac{1}{Gr^{*1/2}} \left( \frac{\partial^2 w^+}{\partial x^{+2}} + \frac{\partial^2 w^+}{\partial y^{+2}} + \delta \frac{\partial^2 w^+}{\partial z^{+2}} \right) - T^+ \end{cases} \quad (11)$$

## 4. Results and Discussion

The results of the differential static pressure profiles ( $\Delta P_{stat}$ ) presented are obtained in steady state according to the reduced Grashof number whose values are represented in table 1. These values are greater than  $10^9$  and the thermal plume can be considered as turbulent.

The experimental static pressure differential measurements were carried out at the CORIA laboratory in France.

**Table 1.** Values of the Grashof numbers reduced depending  $\Delta T_0$ .

$\Delta T_0$ (K)	25	40	60
$Gr^*$	$1.31 \times 10^9$	$2.1 \times 10^9$	$3.47 \times 10^9$

### 4.1. Effect of Grashof Reduced Number on the Differential Static Pressure Profiles

Figure 3 shows the experimental profiles of the static pressure differentials obtained at the position  $x^+ = 0$  and along the depth  $z^+$  of the enclosure. It can be seen in Figure 3 a that the values of the static pressure differential is

almost constant with the increase in the number of the reduced Grashof number for  $z^+$  ranging from 0 to 0.7. When  $z^+$  is between 0.7 and 1, grow this observed. For  $z^+$  varying between 0 and 0.2 the differential profiles of static pressure are decreasing and increasing when  $z^+$  varies from 0.2 to 1 whatever  $Gr^*$ . A  $z^+ = 0.4$  the values of the differential of the static pressure are zero. So this position corresponds to the neutral height. Consequently, the values of the differential of static pressure are negative for the values of  $z^+$  between 0 and 0.4 and positive from 0.4 to 1. It appears from Figure 3b that for the values of  $z^+$  between 0 and 0.9 the values of the differential of static pressure decreases when  $Gr^*$  varies from  $1.31 \times 10^9$  to  $2.1 \times 10^9$  and is almost constant for  $Gr^*$  ranging from  $2.1 \times 10^9$  to  $3.47 \times 10^9$ . For  $z^+$  ranging from 0.9 to 0.94 they are almost constant whatever the values of  $Gr^*$ . When  $Gr^*$  increases, the values of the static pressure differential ( $\Delta P_{stat}$ ) are negative. Figure 3c shows that when  $z^+$  varies from 0 to 0.45 and  $Gr^*$  increases the values of  $\Delta P_{stat}$  decrease. For the values of  $z^+$  ranging between 0.45 and 0.65 the values of  $\Delta P_{stat}$  are quasi constant. For  $z^+$  going from 0.65 to 1, the values of  $\Delta P_{stat}$  increase. For a given value of  $Gr^*$ , the values of

$\Delta P_{stat}$  increase when  $z^+$  varies from 0 to 1. At  $z^+ = 0.6$ ,  $\Delta P_{stat} = 0$  Pa. So the height  $z^+ = 0.6$  is the neutral height. For the values of  $z^+$  varying between 0 and 0.6, the values of  $\Delta P_{stat}$  are negative and positive for the values of  $z^+$  ranging between 0.6 and 1.

The profiles of the static pressure differential decrease and are negative for  $z^+$  ranging from 0 to 0.2. From 0.2 to 1 they increase and are of negative and positive values whatever  $Gr^*$ . For  $Gr^* = 1.31 \times 10^9$ ,  $z^+ = 0.76$ . When  $Gr^* = 2.1 \times 10^9$ ,  $z^+ = 0.66$ . For  $Gr^* = 3.47 \times 10^9$ ,  $z^+ = 0.6$ . At  $z^+ = 0.04$ , the values of  $\Delta P_{stat}$  increase when  $Gr^*$  varies from  $1.31 \times 10^9$  to  $2.1 \times 10^9$  and decrease for  $Gr^*$  going from  $2.1 \times 10^9$  to  $3.47 \times 10^9$ . For  $z^+$  values ranging from 0.095 to the neutral height when the values of  $\Delta P_{stat}$  are negative, the values of  $\Delta P_{stat}$  decrease as  $Gr^*$  increases. From the neutral height to

$z^+ = 1$ , when the values of  $\Delta P_{stat}$  are positive, the values of  $\Delta P_{stat}$  increase as  $Gr^*$  increases.

#### 4.2. Effect of the Number of Openings on the Vertical Differential Static Pressure Profiles

In Figure 3, we remark that the shape of the profiles of the static pressure differential and the neutral height vary according to the number of openings and their positions. The neutral height is lowest in Figure 3b and highest in Figures 3c ( $z^+ = 0.6$ ) and 3d ( $z^+ = 0.6$  to 0.76). It is lower in Figure 3a ( $z^+ = 0.4$ ). The maximum absolute values of static pressure differential are lower in Figure 3d, then Figures 3a and 3c and higher in Figure 3b.

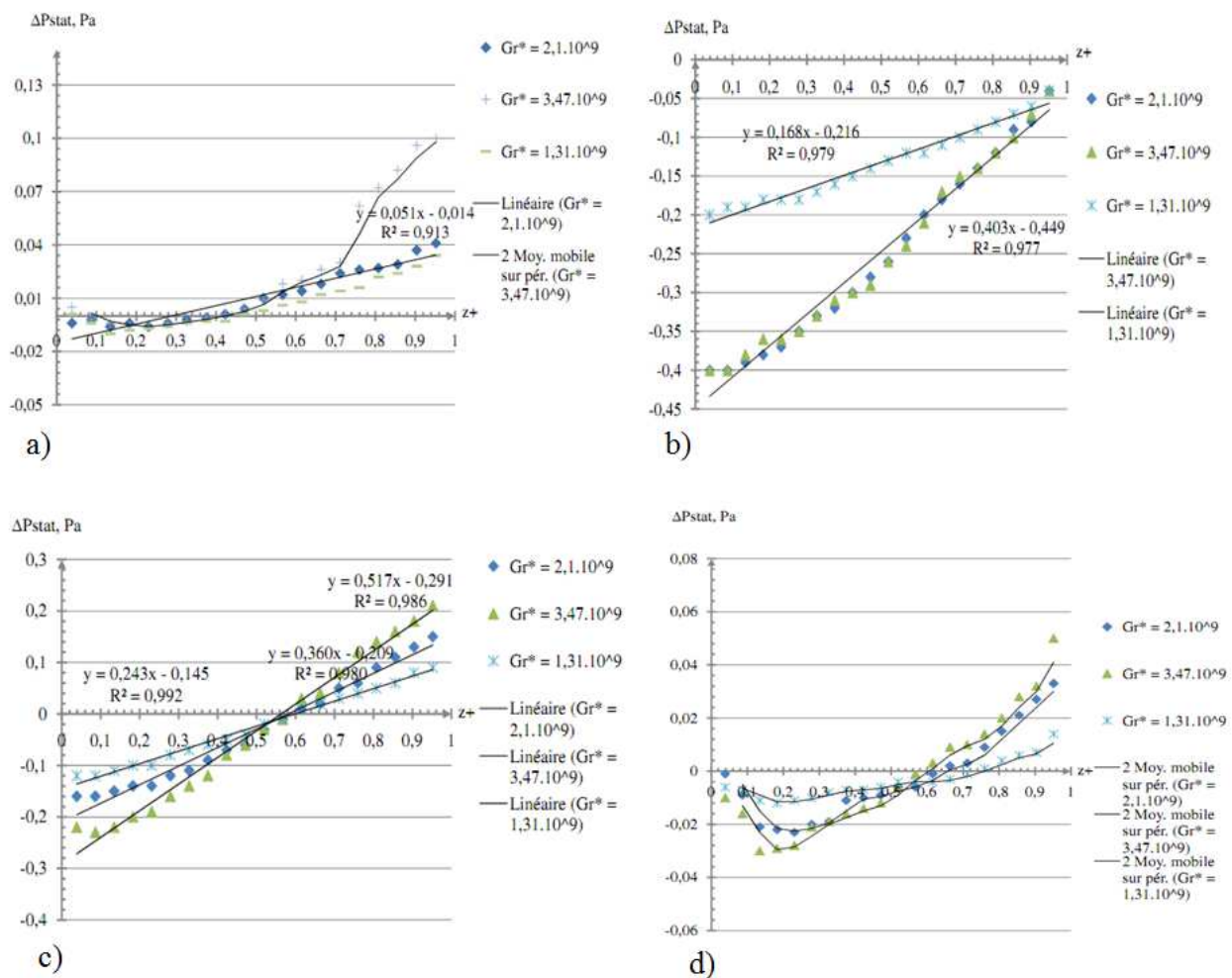


**Figure 3.** Experimental differential static pressure profiles for four geometric configurations of the enclosure as a function of  $Gr^*$  a) case 1, b) case 2, c) case 3 and d) case 4.

#### 4.3. Discussion

In Figure 3 one notices that the values of  $\Delta P_{stat}$ , of maximum  $\Delta P_{stat}$  and of the neutral height vary according to the reduced Grashof number ( $Gr^*$ ), the number of openings and their positions. The neutral height is lower in Figure 3b and the absolute values of the static pressure differential near

the ceiling lower. This implies that there is little air movement at the openings with air entering the enclosure near the bottom of the openings and exiting near the ceiling. In Figure 3a, the neutral height is below the upper openings whose lower parts are at a height  $z^+ = 0.563$ . Consequently, there is air entering the enclosure through the openings located on the floor and leaving through the openings at the



height  $z^+ = 0.596$ . The neutral height  $z^+ = 0.6$  in Figure 3c is located in the openings. Therefore, there is air entering the enclosure near the lower portions of the openings and exiting through the upper portions. In Figure 3d, the neutral height varies between 0.6 - 0.64 ( $Gr^*$  varying between  $2.1 \times 10^9$  and  $3.47 \times 10^9$ ) and 0.76 ( $Gr^* = 1.31 \times 10^9$ ). Therefore, when  $Gr^* = 1.31 \times 10^9$  the air enters the enclosure through the openings located near the floor and at the height  $z^+ = 0.596$  and leaves through the openings located near the ceiling. For  $Gr^*$  varying between  $2.1 \times 10^9$  and  $3.47 \times 10^9$ , the air enters the enclosure through the openings located on the floor and near the lower parts of the openings located at the height  $z^+ = 0.596$  and exits through the upper parts of the openings located at the height  $z^+ = 0.596$  and the openings located near the ceiling.

The difference in static pressure between the inside and the outside of the enclosure is due to the temperature difference between the heat source and the air in the enclosure. This temperature difference creates a density difference inside the enclosure which generates a momentum force with air movement at the openings. The openings allow the enclosure to communicate with the outside environment.

The comparison of these static pressure differential measurements with those of cases 11 and 12 of Kouéni Toko [3], show that the form and the maximum values of the vertical static pressure differential are dependent on the position and the number of openings. For case 4 of our study and that of case 12 of Kouéni Toko [3], the profiles are almost similar and the static pressure differential values are almost identical.

For  $Gr^* = 2.1 \times 10^9$ , the profiles and the values of the differential static pressures of cases 12, 4 and 1 are almost identical.

## 5. Conclusion

Ultimately, it was a question of experimentally studying the static pressure differential profiles generated by a linear heat source in a semi-ventilated enclosure. Four enclosure configurations were chosen, those with two symmetrical openings (Figures 1b and 1c), four openings (Figure 1a) and six openings (Figure 1d). Static pressure differential measurements were made using the Furness control micro-manometer in a large closed room in calm weather. These measurements were made at position  $x^+ = 0$  and according to the depth  $z^+$  of the enclosures at 20 points. We have shown the influences of the reduced Grashof number ( $Gr^*$ ), the number of openings and the position of the openings on the vertical distribution of the differential static pressure profiles with and without dimension. It emerges from this study that the values, the shape of the static pressure vary according to  $Gr^*$ , the number of openings and their positions. The neutral height varies according to the number of openings and their positions but not necessarily according to the  $Gr^*$ . In Figure 3c the neutral height is constant as a function of  $Gr^*$  and varies in Figures 3a and 3d. The difference between the static pressures inside and

outside the enclosure is caused by the temperature difference between the heat source and the air in the enclosure. This temperature difference creates a buoyancy force and then a momentum force. This momentum force generates air movement at the openings between the interior and exterior of the enclosure.

In perspective, we can perform differential static pressure measurements for several positions of the heat source.

## Nomenclature

### Lowercase

$l$	Width Enclosure, m
$x$	Longitudinal coordinate, m
$y$	Vertical coordinate, m
$z$	Transverse coordinate, m
$u$	Horizontal component of the velocity, $m.s^{-1}$
$v$	Vertical component of the velocity, $m.s^{-1}$
$w$	Transverse velocity component, $m.s^{-1}$
$cte$	Constant

### Capital Letters

$L$	Enclosure length, m
$H$	Enclosure height, m
$\Delta T_0$	Temperature difference between the heat source and the outside, K
$T$	Temperature inside the enclosure, K
$T_0$	Temperature of the heat source, K
$U_0$	Maximum inlet gas velocity in the enclosure, K
$P$	Static pressure inside enclosure, Pa
$P_{max}$	Maximum static pressure inside enclosure, Pa
$\Delta P_{stat}$	Static pressure difference between inside and outside enclosure, Pa

### Greek Symbols

$\nu$	Kinematic viscosity of air, $m^2.s^{-1}$
$\rho$	Density, $kg.m^{-3}$
$\beta$	Coefficient of thermal expansion, $K^{-1}$
$\rho_{ext}$	Density of gases outside of the enclosure, $kg.m^{-3}$

### Dimensionless Numbers

$Pr$	Prandtl number
$Gr$	Grashof number

### Special Characters

$Gr^*$	Reduced Grashof number
$x^+$	Dimensionless longitudinal coordinate
$y^+$	Dimensionless vertical coordinate
$z^+$	Coordinated transverse to size
$u^+$	Horizontal component of the dimensionless velocity
$v^+$	Vertical component of the dimensionless velocity
$w^+$	Transverse component of the dimensionless velocity
$P^+$	Static pressure to size
$T^+$	Temperature to size
$\delta$	Aspect Ratio

## Acknowledgements

I thank the CORIA's laboratory for the implementation of the experiment.

## References

- [1] Linden P. F., Lane-Serff G. F., Smeed D. A. (1990) Emptying filling boxes: the fluid mechanics of natural ventilation, *Journal of Fluid Mechanics*, 212, 309–335.
- [2] Kaye N. B. and Hunt G. R. (2004) Time-dependent flows in an emptying filling box, *Journal of Fluid Mechanics*, 520, 135–156.
- [3] Koueni Toko C. A. (2019) Etude des champs dynamique et thermique dans une enceinte semi-ventilée en convection naturelle, *Rapport annuel de thèse-CORIA*.
- [4] Kouéni-Toko C. A., Tcheukam-Toko D., Kuitche A., Patte-Rouland B., Paranthoën P. (2020) Numerical modeling of the temperature fields in a semi-confined enclosure heated by a linear heat source, *International Journal of Thermofluids*, Vol. 7–8, 100017.
- [5] Mahmud H. Ali, Rawand E. Jalal (2020) Natural convection in a square enclosure with different openings and involves two cylinders: a numerical approach, *Frontiers in Heat and Mass Transfer*, 15, 27.
- [6] Gladstone C. and Woods A. W. (2001) On buoyancy-driven natural ventilation of a room with a heated floor, *Journal of Fluid Mechanics*, 441, 293–314.
- [7] Kaye N. B., Hunt G. R. (2007) Overturning in a filling box, *Journal of Fluid Mechanics*, 576, 297–323.
- [8] Jun Fang, Hong-Yong Yuan (2007) Experimental measurements, integral modeling and smoke detection of early fire in thermally stratified environments, *Fire Safety Journal*, 42, 11–24.
- [9] Fitzgerald S. D. and Woods A. W. (2010) Transient natural ventilation of a space with localized heating, *Building and Environment*, 45, 2778–2789.
- [10] Jeremy C. P. and Andrew W. W. (2004) On ventilation of a heated room through a single doorway, *Building and Environment*, 39, 241–253.
- [11] Paranthoën P. and Gonzalez M. (2010) Mixed convection in a ventilated enclosure, *International Journal of Heat and Fluid Flow*, 31, 172–178.
- [12] Lucchesi C. (2009) Etude du mouvement d'un fluide de faible masse volumique entre deux compartiments reliés par une ouverture de type porte: Application à la propagation de la fumée d'incendie, *Thèse Mécanique des fluides Aix Marseille II-France*.
- [13] Decheng Li (2018) Transport phenomena of fire-induced smoke flow in a semi-open vertical shaft, *International Journal of Numerical Methods for Heat & Fluid Flow*, 28, 2664–2680.
- [14] R. Harish (2019) Buoyancy driven turbulent plume induced by heat source in vented enclosure, *International Journal of Mechanical Sciences*, 148, 209–222.
- [15] José Luis Fernández-Zayas, Juan Francisco Villa-Medina, Norberto Chargoy-del Valle, Miguel Àngel Porta-Gándara (2022) Experimental analysis of natural ventilation of an office building in Mexico city, *Case Studies in Thermal Engineering*, Vol. 28, 101661.
- [16] Fitzgerald Shaun D., Woods A. W. (2004) Natural ventilation of a room with vents at multiple levels, *Building and Environment*, 39, 505–521.